

## Pb(II) Effect on Electrosynthesis of Lead Dioxide in Alkaline Solution

Shiwei He<sup>1,2</sup>, Ruidong Xu<sup>1,2,\*</sup>, Sha Han<sup>1</sup>, Jiong Wang<sup>1</sup>, Buming Chen<sup>1</sup>

<sup>1</sup> Faculty of Metallurgical and Energy Engineering, Kunming University of Science and Technology, Kunming 650093, China;

<sup>2</sup> State Key Laboratory of Complex Nonferrous Metal Resources Cleaning Utilization, Kunming 650093, China.

\*E-mail: [rdxupaper@aliyun.com](mailto:rdxupaper@aliyun.com)

Received: 24 January 2016 / Accepted: 13 April 2016 / Published: 4 May 2016

---

An electrochemical investigation focused on electrosynthesis of lead dioxide in alkaline solutions, using rotating disk electrode (RDE) and rotating ring disk electrode (RRDE), has been carried out. The experiments show that Pb(II) haven't modified the evolution of oxygen in alkaline solutions, and the reaction taking place at 0.6 V<sub>SCE</sub> is under the mixed control of ionic transport and charge transfer. Koutechy-Levich equation has been used to calculate the value of diffusion coefficient D and apparent heterogeneous rate constant *k* of Pb(II) oxidation reaction at 0.6 V<sub>SCE</sub>. The calculation results indicate that Pb(II) itself has the negative influence on the diffusion of Pb(II). In addition, Pb(II) has the positive influence on the apparent heterogeneous rate constant of PbO<sub>2</sub> electrodeposition process. The intermediate was discovered in PbO<sub>2</sub> electrodeposition process using RRDE. XRD and SEM were employed to investigate the phase composition and surface microstructure of the synthesized deposit. The result confirms that PbO<sub>2</sub> synthesized in an alkaline solution consists of pure  $\alpha$  phase, but not all characteristic peaks are present and relative intensities are not in agreement with the ICDD card. The deposit shows the preferential orientation of growth in the (200) crystallographic plane, and the deposit is compact and uniform which is composed of rounded nanocrystallites.

---

**Keywords:** lead dioxide; alkaline solution; Pb(II) concentration; RDE; RRDE

### 1. INTRODUCTION

Lead dioxide (PbO<sub>2</sub>) has attracted considerable attentions owing to its low electrical resistivity, low cost, ease of preparation, good chemical stability in acid media, high overpotential for the oxygen evolution reaction (OER) and relatively large surface area [1-4]. Thus, lead dioxide has already been used in, waste water treatment [5-7], ozone generation [8,9], batteries [10-12], analytical sensors [13] and electrowinning process [14].

As we all known, lead dioxide have two phases:  $\alpha$  phase and  $\beta$  phase. Electrodeposition is a traditional way to prepare this two phases of  $\text{PbO}_2$  [15]. The conditions (mainly composition and temperature) of the synthesizing bath determine the phase of the deposits [16]. To our best knowledge,  $\alpha$ - $\text{PbO}_2$  is less studied than  $\beta$ - $\text{PbO}_2$  due to its lower electrochemical activity and electrical conductivity [17]. Despite the shortcomings mentioned above,  $\alpha$ - $\text{PbO}_2$  is chemically more stable than  $\beta$ - $\text{PbO}_2$ ; consequently, it promotes longer life cycles of lead-acid batteries [18]. In addition, it is beneficial to ozone production [19], presents the same performance of  $\beta$ - $\text{PbO}_2$  as pH sensor [20] and is the first step of the electrochemical fabrication of metallic lead nanowires (NWs) [21]. What's more, as an interlayer of the electrode, the binding force of  $\beta$ - $\text{PbO}_2$  and underlayer would be improved by  $\alpha$ - $\text{PbO}_2$  [22].

Cyclic voltammetry (CV) technology is a general and powerful method to study reactions in aqueous solutions, surface adsorption and deposition [23,24]. It can be used to investigate the kinetics of charge transfer at the electrode/electrolyte interface, when paired with a rotating disk electrode (RDE) [25–29]. The current generated by an electrochemical process under a given potential gradient is determined by two parts. The one is transport of reactant ions to the electrode and the other is kinetics of its conversion at the electrode surface. Rotating disk electrode can easily establish a steady-state condition. At this condition, the Koutecky-Levich equation can express the relative contribution of mass transport and kinetics (in terms of resistance to charge transfer) to the current generated at an RDE experiment [30,31].

In this present work, we studied and carried out the effect of  $\text{Pb(II)}$  concentration on electrodeposition of lead dioxide in alkaline solutions. In these conditions, the value of diffusion coefficient  $D$  and apparent heterogeneous rate constant  $k$  of the  $\text{PbO}_2$  electrodeposition process were calculated by Koutecky-Levich equation. And the effect of  $\text{Pb(II)}$  concentration on the kinetic parameters  $D$  and  $k$  have been carried out. The phase composition and surface microstructure of deposit synthesized on a platinum surface have been carried out by means of XRD and SEM, respectively. These research results are helpful to provide the theoretical basis and technical support for the preparation of  $\text{PbO}_2$  in alkaline solutions.

## 2. EXPERIMENTATION

### 2.1. Cyclic voltammetry and rotating disk electrode

The cyclic voltammetry experiments were carried out using aqueous solutions of  $\text{Pb(II)}$  and  $\text{NaOH}$  at certain ratios. Alkaline solutions were prepared by dissolving litharge ( $\text{PbO}$ ) in  $\text{NaOH}$  solution and the  $\text{NaOH}$  concentration were controlled at 3.5 M. Analytical grade reagents (AR) and twice distilled water were used for all solutions. High purity nitrogen gas was purged into the solutions before applying the potential. The temperature of experiments were controlled at 30 °C. A three-electrode system was employed. The working electrode was a Pt RDE (Ametek) with an exposed Pt area of 0.196 cm<sup>2</sup> mounted to a rotator. A platinum electrode was the counter electrode and a saturated calomel electrode (SCE) was the reference one. The reference electrode and working electrode were

linked by luggin capillary filled with agar and potassium chloride. In addition, the distance between capillary and working electrode surface was about 4d (d is the diameter of capillary). Cyclic voltammetry curves and anodic polarization curves were obtained using an electrochemical workstation (PARSTAT2273). All the potentials were given against the SCE.

## 2.2. Rotating-ring disk electrode

The rotating ring disk electrode (RRDE) used in the experiment was a Pt ring and Pt disk electrode, which was produced by Ametek. CHI900C electrochemical workstation was employed to supply two different potentials on Pt ring and Pt disk. A platinum electrode was the counter electrode and a saturated calomel electrode (SCE) was the reference one. The reference electrode and working electrode were linked by luggin capillary filled with agar and potassium chloride. In addition, the distance between capillary and working electrode surface was about 4d (d is the diameter of capillary). The rotating speed of RRDE was controlled at 1000 rpm and the potential of ring is controlled at -0.4 V against SCE. The temperature of experiments were controlled at 30 °C.

## 2.3. Apparent heterogeneous rate constant and diffusion coefficient

Values of the apparent heterogeneous rate constants (k) and diffusion coefficients (D) for Pb(II) oxidation were calculated from the linear plots of  $I^{-1}$  versus  $\omega^{-1/2}$  according to the Koutecky-Levich equation:

$$I^{-1} = (0.62nFAD^{2/3}\nu^{-1/6}C\omega^{1/2})^{-1} + (nFAkC)^{-1} \quad (1)$$

Where  $\omega$  is the angular velocity of Pt-RDE (rad/s), C is the bulk concentration of the reacting species (mol/m<sup>3</sup>),  $\nu$  is the kinematic viscosity of the solution (m<sup>2</sup>/s), F is the Faraday constant (C/mol), A is the surface area of Pt-RDE (m<sup>2</sup>), and n is the effective number of electrons exchanged in the reaction. The rate constants (k) and diffusion coefficients (D) were measured at E=0.6 V. Kinematic viscosity ( $\nu$ ) was calculated by the equation:

$$\nu = \mu / \rho \quad (2)$$

where  $\mu$  is the dynamic viscosity of the solution (Pa·s), and  $\rho$  is the density of the solution (kg/m<sup>3</sup>). The dynamic viscosity ( $\mu$ ) was measured by Brookfield viscometer, and the density was the ratio of mass and volume, which were measured by normal method.

## 2.4. Characterization of surface and phase composition

The phase composition and surface microstructure characteristics of PbO<sub>2</sub> synthesized on Pt-RDE were measured by D/Max-2200 X-ray diffractometer (XRD) and Nova NanoSEM450 scanning electron microscope (SEM), respectively. The sample was prepared by potentiostatic polarization (0.6 V) in the solution of 3.5 M NaOH and 0.15 M Pb(II). The synthesis time was controlled at 2 h and temperature was 30 °C.

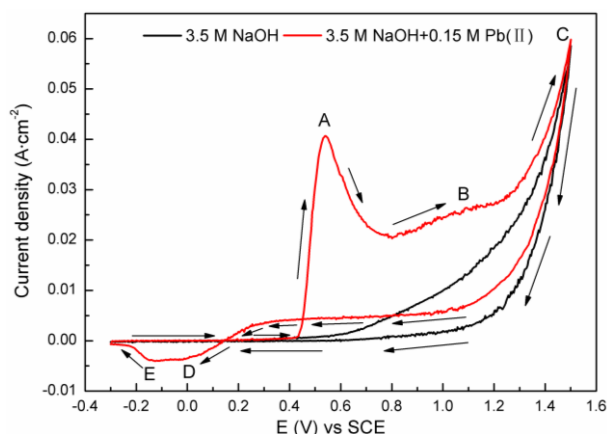
### 3. RESULTS AND DISCUSSION

#### 3.1. Cyclic voltammetry study

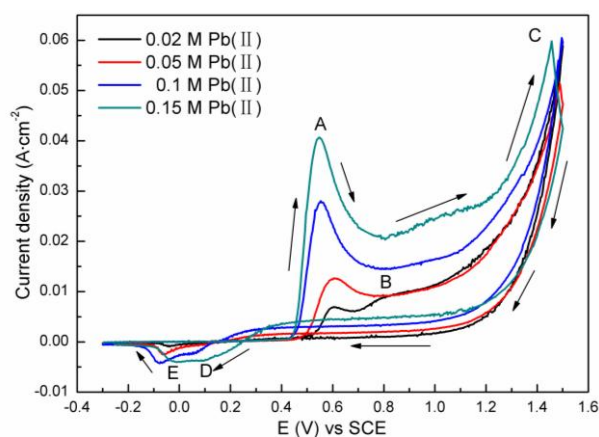
Voltammograms measured in the solution of 3.5 M NaOH + 0.15 M Pb(II) and blank solution (3.5 M NaOH) at 30 °C are shown in Fig. 1. There are only one peak in the blank curve, which can be related to the oxygen evolution. All peaks related to the solution containing Pb(II) are referred to with letters. Five main peaks (A to E) can be detected on the curve of Pb(II) containing solution. On the anodic branch of the curve, peak C is corresponding to the oxygen evolution. Peak A is seems to be the process of Pb(II) oxidation, but the product of the oxidation process is not clear.  $\text{Pb(II)} \rightarrow \text{PbO}_2$  or  $\text{Pb(II)} \rightarrow \text{Pb}_3\text{O}_4$  may both exist in the process, but the front one is the main reaction. Compared with reference [32], the potential of Pb(II) oxidation in alkaline solution is lower than acidity solution. In the potential range of 0.75~1.2 V, the current density is stable, and the  $\text{PbO}_2$  electrosynthesis occurred simultaneously with oxygen evolution in this range. So Peak B is a mixed peak, which is consist of the oxygen evolution and  $\text{Pb(II)} \rightarrow \text{PbO}_2$ . On the cathodic branch, peak D and E correspond most likely to the process of  $\text{PbO}_2 \rightarrow \text{Pb}_3\text{O}_4$  and  $\text{PbO}_2 \rightarrow \text{Pb(II)}$ , respectively. The intensity of peak A and E are not in the same order of magnitude, indicating that the reaction ( $\text{Pb(II)} \rightarrow \text{PbO}_2$ ) is an irreversible process. The two curves almost coincide with each other in the high potential range of oxygen evolution, but they doesn't coincide in the potential range of 0.4~1.3 V which would caused by the continuous formation of  $\text{PbO}_2$  in Pb(II) containing solution. The conclusion can be draw that the presence of Pb(II) haven't modified the evolution of oxygen.

Fig. 2 shows the effect of varying the concentration of Pb(II) as well as the potential scan range (NaOH controlled at 3.5 M). The intensity of peak A is the expected increase as the Pb(II) concentration increased and the increase in intensity is proportional to the change in Pb(II) concentration. This phenomenon confirmed that peak A is mainly reflect to the Pb(II) oxidation. In the potential range of 0.8~1.1 V,  $\text{PbO}_2$  continuous generated on the electrode simultaneously with the oxygen evolution, which can be observed from Fig.1. The intensity of this range obtained in 0.02 M Pb(II) oxidation and 0.05 M Pb(II) are close. One possible explanation is that the Pb(II) concentration is very low so as to the proportion of Pb(II) oxidation in the range, which means that the main reaction in the range is mainly oxygen evolution obtained in Pb(II) concentration of 0.02 M and 0.05 M. As Pb(II) concentration increased to 0.1 M and 0.15 M, the current proportion of Pb(II) oxidation increased in this potential range, as a consequence the current of the range increased. The mixed peak B become not obvious as Pb(II) concentrated in the solution. The increasing proportion of Pb(II) oxidation in the stable potential range can give an explanation. As cathodic peaks, peaks D and E can also reflect the whole formation weight of the  $\text{PbO}_2$  generated in the anodic scan, the similar analytical skill has been widely used in the papers written by A.B. Velichenko. Peak D is not obvious in the curves obtained in solutions containing 0.02 M Pb(II) and 0.05 M Pb(II). Moreover, the intensity of peak E increased follows as Pb(II) concentrated in the Pb(II) range of 0.02~0.1 M. However, intensity of peak E obtained in 0.15 M Pb(II) is close to peak E obtained in 0.1 M Pb(II) containing solution. As peak A of 0.15 M Pb(II) is larger than 0.1 M Pb(II), the formation weight of the generated  $\text{PbO}_2$  in the anodic scan is much more than 0.1 M Pb(II). But the cathodic peak E obtained in solutions of the two

Pb(II) concentrations is similar. The reason for this phenomenon mentioned above is that the  $\text{PbO}_2$  generated in the solution containing 0.15 M Pb(II) is harder to be reduced, compared with the  $\text{PbO}_2$  generated in the solution containing 0.1 M Pb(II).



**Figure 1.** Cyclic voltammogram of a Pt electrode in 3.5 M NaOH + 0.15 M Pb(II) solution at 30 °C, in comparison with a blank solution ( $v=50$  mV/s)



**Figure 2.** Cyclic voltammogram of a Pt electrode in solutions of different Pb(II) concentrations, NaOH controlled at 3.5 M ( $v=50$  mV/s)

### 3.2. Rotating disk electrode study

Fig. 3 shows the anodic polarization curves of a solution containing different Pb(II) (NaOH controlled at 3.5 M) with a scan rate of 50 mV/s and different rotating speeds, varying from 400 to 2000 rpm. The whole four graphs of Fig.3 show almost the identical features. There are no reaction existing in the potential range of 0~0.43 V, after 0.43 V the intensity starts to increase, the intensity reached to a stable region at about 0.55~0.85 V. Some curves obtained in the high Pb(II) containing solutions (0.1 M and 0.15 M) with high rotation speed are disordered at the potential range about 0.9~1.2 V. It is because that the blinding force of  $\text{PbO}_2$  and Pt substrate is not very strong so that the generated  $\text{PbO}_2$  would exfoliated from substrate. The measured dependences of intensity at stable

region are obvious at different rotation speed. This result is unambiguous evidence that the transport (mass transfer) of Pb(II) to the electrode surface limit the rate of the electrode process.

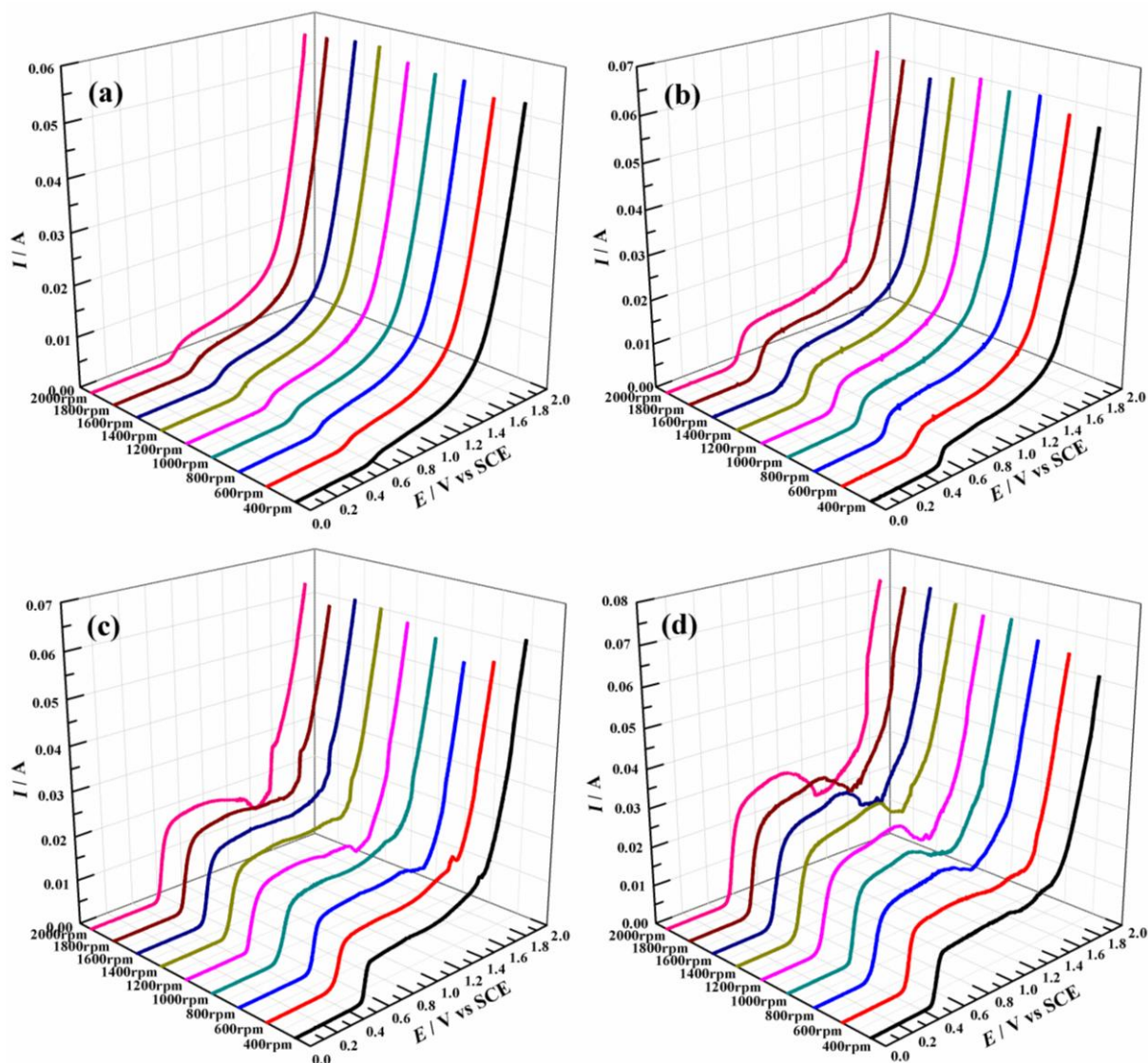


**Figure 3.** Anodic polarization curves of a Pt RDE in solutions of different Pb(II) concentrations and rotating speeds, (a): 0.02 M Pb(II), (b): 0.05 M Pb(II), (c): 0.1 M Pb(II), (d): 0.15 M Pb(II), NaOH controlled at 3.5 M ( $v=50$  mV/s)

Fig. 4 shows the Koutechy-Levich plot obtained at diffusion plateau (0.6 V) of different Pb(II) concentrations. The curves indicate that there is direct proportionality between  $I^{-1}$  and  $\omega^{-1/2}$ , and the intercept on I axes is not zero. A result can be drawn that a mixed control (ion transport and kinetics) existed in the reaction taking place at 0.6 V [30,33]. A line has been fitted through the points obtained and fitting goodness of each line is shown in Figure. 4. The diffusion coefficient  $D$  has been calculated from the value of the slope, using Eq.(1) above. The values of the parameters used in the equation and the results of all calculations are shown in Table 1: all the parameters are experimental. It has been

assumed that the reaction taking place at 0.6 V is Pb(II)→Pb(IV) (hence  $n=2$ ). The apparent heterogeneous rate constant  $k$  has also been calculated, from the value of the intercept of the fitted line. The diffusion coefficient  $D$  and apparent heterogeneous rate constant  $k$  have obviously relationship with Pb(II) concentration in the solution. The value of diffusion coefficient decreased as the Pb(II) concentrated, which indicates that Pb(II) itself have the negative influence on the diffusion of Pb(II) at Pb(II) concentration range of 0.02~0.15 M. It means that Pb(II) has competitive relation with other Pb(II) in the process of diffusing to the electrode surface. On the other hand, the value of the apparent heterogeneous rate constant  $k$  increased as the Pb(II) concentrated at Pb(II) concentration range of 0.02~0.15 M. Formula (3) is the main reaction of PbO<sub>2</sub> electrodeposition in alkaline solutions [34~36]. Pb(II) in the alkaline solution is mainly existed as HPbO<sub>2</sub><sup>-</sup>[37]. The result shows that HPbO<sub>2</sub><sup>-</sup> ions have the positive influence on the process of PbO<sub>2</sub> electrodeposition, but 0.15 M Pb(II) is almost saturated in 3.5 M NaOH solution. So the Pb(II) concentration should be improved as much as possible in the alkaline solutions, in order to promoting PbO<sub>2</sub> electrodeposition.

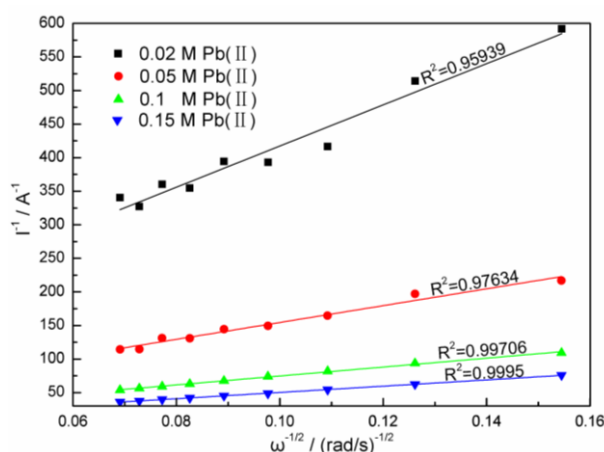
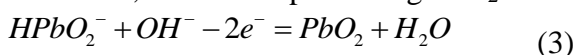


**Figure 4.** Koutecky-Levich plot obtained at diffusion plateau (0.6 V) of different Pb(II) concentrations

**Table 1.** Verification of Koutecky-Levich equation

Pb(II) Concentration	Koutecky-Levich equation: $I^{-1}=(0.62nFAD^{2/3}v^{-1/6}C\omega^{1/2})^{-1}+(nFAkC)^{-1}$							
	$nF(C/mol)$	$C(mol/m^3)$	$A(m^2)$	$v(m^2/s)$	Intercept	Slope	$k(m/s)$	$D(m^2/s)$
0.02 M	1.93E+09	20	1.96E-05	3.78E-06	110.66	3068.13	1.19E-04	8.06E-10
0.05 M	1.93E+09	50	1.96E-05	3.98E-06	29.02	1254.13	1.82E-04	7.85E-10
0.1 M	1.93E+09	100	1.96E-05	4.04E-06	8.43	663.29	3.14E-04	7.29E-10
0.15 M	1.93E+09	150	1.96E-05	4.26E-06	3.58	466.73	4.93E-04	6.81E-10

### 3.3 Rotating ring-disk electrode study

The anodic polarization curves of a Pt RRDE in the solutions of different Pb(II) concentrations are shown in Fig. 5. The upside of Fig. 5 reveals the current generated on the Pt disk electrode and the downside reveals the current generated on the Pt ring electrode when the ring potential was controlled at  $-0.4$  V.  $I_R$  shows one peak obtained in the solution without Pb(II). So this peak is caused by the reduction of soluble oxygen generated on the Pt disk electrode. As Pb(II) added to the solution, there are two peaks existing in the  $I_R$  part. The peaks at more positive potential is corresponding to the reduction of soluble oxygen mentioned above. In addition, the peaks at more negative potential should be attributed to the reduction of soluble Pb(III) or Pb(IV), which were generated in the electrodeposition process of  $PbO_2$  formation. This means that the process explained by formula (3) is not finished by one step. It must generate an soluble intermediate (Pb(III) or Pb(IV)) first, then deposit on the surface of the disk by formation of  $PbO_2$ . The similar conclusion was obtained by Colin J. Clarke[38] in research on the electrodeposition of  $MnO_2$  using RRDE. They find out soluble intermediate also existing in  $MnO_2$  electrodeposition process in acidity solution. The intensity of peak at more negative potential increase as Pb(II) concentration increased at the Pb(II) region of 0.02~0.1 M, then decrease at the Pb(II) region of 0.1~0.15 M. This indicate that the formation weight of intermediate increased follows the increasing of Pb(II) in the solution at the Pb(II) region of 0.02~0.1 M. However, as Pb(II) concentration increased to 0.1 M, the formation weight of intermediate starts to decrease. Lowering the formation weight of intermediate can improve the proportion of one step electrodeposition in the  $PbO_2$  formation process. The conclusion can be drawn that the increasing of Pb(II) concentration have positive influence on inhibiting the formation of intermediate and improving the proportion of one step electrodeposition of  $PbO_2$ . This may be a reasonable explanation to the phenomenon mentioned in section 3.2 that the apparent heterogeneous rate constant  $k$  increase as Pb(II) concentrated in the solution.

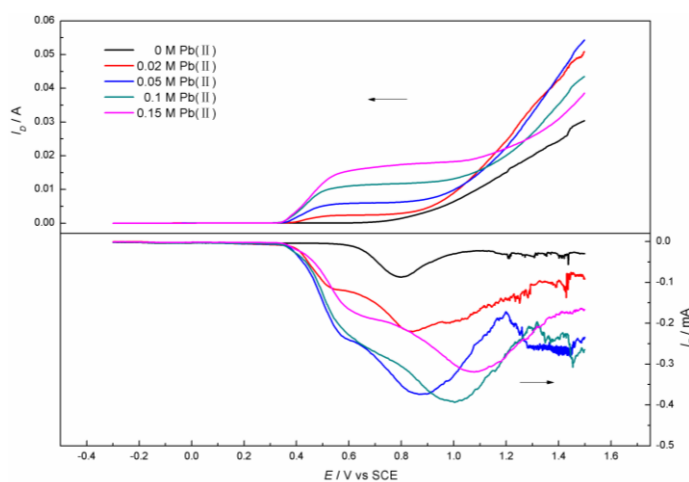


**Figure 5.** Anodic polarization curves of a Pt RRDE in solutions of different Pb(II) concentrations, NaOH controlled at 3.5 M (Rotating speed: 1000 rpm;  $E_R = -0.4$  V;  $v = 50$  mV/s)



### 3.4. Phase compositions and surface microstructures

The XRD patterns of deposit synthesized on Pt electrode surface in solution of 0.15 M Pb(II) and 3.5 M NaOH are shown in Fig. 6. XRD analysis confirms that PbO<sub>2</sub> synthesized in the alkaline solution consists of pure  $\alpha$  phase, matching the card 72-2440 of ICDD database [39]. However, not all characteristic peaks are present and relative intensities are not in agreement with the ICDD card, which was also observed in [40]. A preferential orientation of growth in the (200) crystallographic plane can easily be observed, and the  $\alpha$ -PbO<sub>2</sub> deposit is polycrystalline. Compared to (200) crystallographic plane, the intensity of other crystallographic plane is so much lower. The average crystallite size (Lhkl) of synthesized  $\alpha$ -PbO<sub>2</sub> was estimated from the full width at half maximum height (FWHM) of the peak at 36.2°. Debye-Scherrer equation, which is valid for nanosized crystallites, was employed in the estimation, and the calculated average crystallite of the condition is 33.3 nm. Fig. 7 shows the SEM images of PbO<sub>2</sub> synthesized on Pt electrode surface in solution of 0.15 M Pb(II) and 3.5 M NaOH. As can be seen, compact and uniform deposit were obtained in this synthesizing condition and the deposit is composed of rounded nanocrystallites.

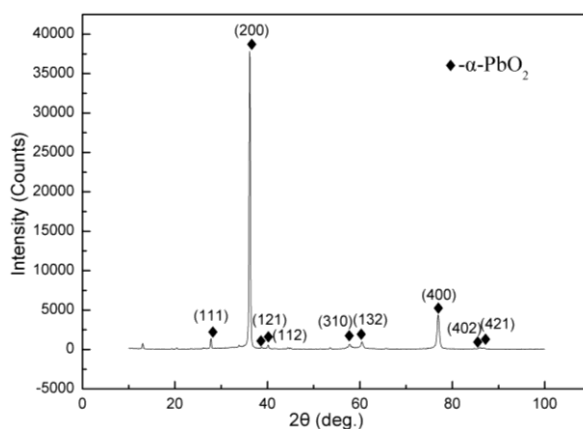


**Figure 6.** XRD patterns of deposit synthesized on Pt electrode surface in solution of 0.15 M Pb(II) and 3.5 M NaOH

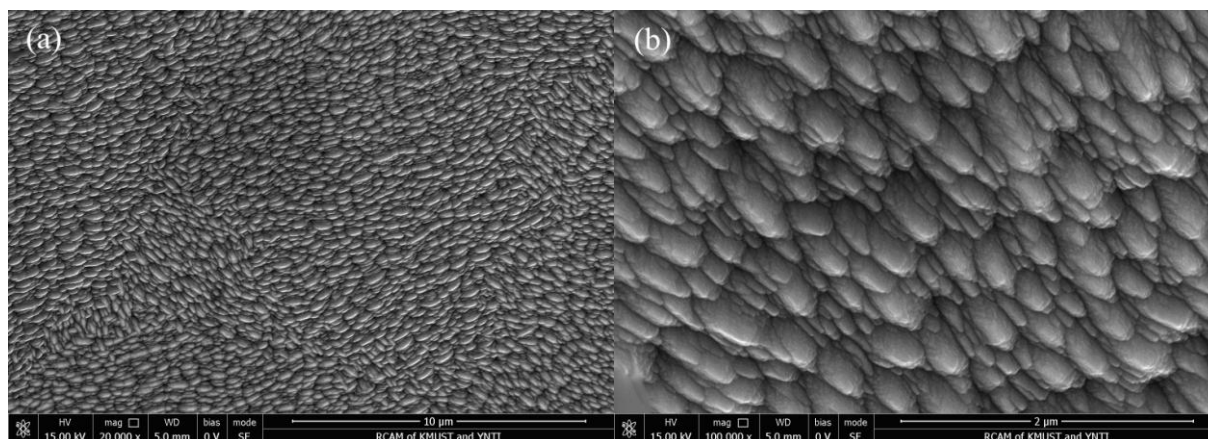


**Figure 7.** SEM images of deposit synthesized on Pt electrode surface in solution of 0.15 M Pb(II) and 3.5 M NaOH (a: 20000 $\times$ ; 100000 $\times$ )

#### 4. CONCLUSIONS

In this study, the effect of Pb(II) concentration were investigated by cyclic voltammetry and rotating disk electrode techniques, in order to study the electrodeposition process affected by Pb(II). The presence of Pb(II) haven't modified the evolution of oxygen in alkaline solutions, and the reaction taking place at 0.6 V is under the mixed control of ionic transport and charge transfer. The value of diffusion coefficient  $D$  and apparent heterogeneous rate constant  $k$  of electrodeposition process at 0.6 V were calculated by Koutechy-Levich equation. The value of diffusion coefficient decreased as the Pb(II) concentrated, which indicates that Pb(II) itself have the negative influence on the diffusion of Pb(II) at Pb(II) concentration range of 0.02~0.15 M. The value of the apparent heterogeneous rate constant  $k$  increased as the Pb(II) concentrated, which indicates that Pb(II) have the positive influence on the process of PbO<sub>2</sub> electrodeposition. So the Pb(II) concentration should be improved as much as possible in the alkaline solutions, in order to promoting PbO<sub>2</sub> electrodeposition. The RRDE investigation was used to confirm whether the intermediate was existed in the process. The result shows that soluble intermediate was indeed existed in PbO<sub>2</sub> electrodeposition process. In addition, the increasing of Pb(II) concentration have positive influence on inhibiting the formation of intermediate and improving the proportion of one step electrodepostion of PbO<sub>2</sub>. The deposit was obtained on the platinum electrode surface, via anodic galvanostatic polarization at 10 mA/cm<sup>2</sup> in the solution of 0.15 M Pb(II) and 3.5 M NaOH. XRD and SEM were employed to investigate the deposit. XRD analysis confirms that PbO<sub>2</sub> synthesized in an alkaline solution consists of pure  $\alpha$  phase, but not all characteristic peaks are present and relative intensities are not in agreement with the ICDD card. The deposit shows the preferential orientation of growth in the (200) crystallographic plane, and the deposit is compact and uniform which is composed of rounded nanocrystallites.

#### ACKNOWLEDGEMENT

Authors gratefully acknowledge the financial supports of the Specialized Research Fund for the Doctoral Program of the Ministry of Education of China (Project No.20125314110011); the Key Project of Yunnan Province Applied Basic Research Plan of China (Project No.2014FA024); the National Natural Science Foundation of China (Project No.51564029).

#### References

1. A.M. Couper, D. Pletcher, and F.C. Walsh, *Chem. Rev.*, 90 (1990) 837
2. H. Yang, B. Chen, H. Liu, Z. Guo, Y. Zhang, X. Li, and R. Xu, *Int. J. Hydrogen Energy*, 39 (2014) 3087
3. M. Panizza, I. Sirés, and G. Cerisola, *J. Appl. Electrochem.*, 38 (2008) 923
4. L. Chang, Y. Zhou, X. Duan, W. Liu, and D. Xu, *J. Taiwan Inst. Chem. E.*, 45 (2014) 1338
5. D.C. Johnson, J. Feng, and L.L. Houk, *Electrochim. Acta*, 46 (2000) 323
6. H. An, Q. Li, D. Tao, H. Cui, X. Xu, L. Ding, and J. Zhai, *Appl. Surf. Sci.*, 258 (2011) 218
7. J. Xing, D. Chen, W. Zhao, X. Zhao, and W. Zhang, *RSC Adv.*, 66 (2015) 53504
8. R. Amadelli, L. Armelao, A.B. Velichenko, N.V. Nikolenko, D.V. Girenko, S.V. Kovalyov, and F.I. Danilov, *Electrochim. Acta*, 45 (1999) 713
9. J. Wu, H. Xu, and W. Yan, *RSC Adv.*, 25 (2015) 19284

10. H.Y. Chen, L. Wu, C. Ren, Q.Z. Luo, Z.H. Xie, X. Jiang, and Y.R. Luo, *J. Power Sources*, 95 (2001) 108
11. W. Yang, W. Yang, and X. Lin, *Appl. Surf. Sci.*, 258 (2012) 5716
12. W. Zhang, H. Lin, H. Kong, H. Lu, Z. Yang, and T. Liu, *Int. J. Hydrogen Energy*, 39 (2014) 17153
13. D. Velayutham, and M. Noel, *J. Appl. Electrochem.*, 23 (1993) 922
14. C.J. Yang, and S.M. Park, *Electrochim. Acta*, 108 (2013) 86
15. H. Bode, *Lead-Acid Batteries*, Wiley, New York (1977)
16. D. Devilliers, T. Dinh, E. Mahé, V. Dauriac, and N. Lequeux, *Electroanal. Chem.*, 573 (2004) 227
17. B. Chen, Z. Guo, H. Huang, X. Yang, and Y. Cao, *Acta Metall. Sin.*, 22 (2009) 373
18. A.J. Salkind, A.G. Cannone, and F.A. Trumbure, *Hand-book of Batteries*, McGraw-Hill, New York (2002)
19. K. Kinoshita, *Electrochemical Oxygen Technology*, Wiley, New York (1992)
20. A. Eftekhari, *Sens. Actuators B*, 88 (2003) 234
21. R. Inguanta, E. Rinaldo, S. Piazza, and C. Sunseri, *Electrochem. Solid State Lett.*, 13 (2010) K1
22. S. He, R. Xu, G. Hu, and B. Chen, *Electrochemistry*, 83 (2015) 974
23. K. Polat, M.L. Aksu, and A.T. Pekel, *J. Appl. Electrochem.*, 32 (2002) 217
24. R. Wartena, J. Winnick, and P.H. Pfromm, *J. Appl. Electrochem.*, 32 (2002) 725
25. G. Prentice, *Electrochemical Engineering Principles*, Prentice Hall (1991)
26. J.M. Maciel, and S.M.L. Agostinho, *J. Appl. Electrochem.*, 30 (2000) 981
27. A. Neville, T. Hodgkiess, and A.P. Morizot, *J. Appl. Electrochem.*, 29 (1999) 455
28. J.O.M. Bockris, and A.K.N. Reddy, *Electrochim. Acta*, 22 (1977) 41
29. A.J. Bard, and L.R. Faulkner, *Electrochemical Methods: Fundamentals and Applications*, Wiley, New York (2001)
30. P.A. Christenses, and A. Hamnett, *Techniques and Mechanisms in Electrochemistry*, Springer Science & Business Media (1994)
31. F. Brusciotti, and P. Duby, *Electrochim. Acta*, 52 (2007) 6644
32. A. B. Velichenko, R. Amadelli, E. V. Gruzdeva, T. V. Luk'yanenko, and F. I. Danilov, *J. Power Sources*, 191 (2009) 103
33. T.D. Cabelka, D.S. Austin, and D.C. Johnson, *J. Electrochem. Soc.*, 131 (1984) 1595
34. B. Chen, Z. Guo, and X. Yang, *China Nonferrous Metallurgy*, B2 (2009) 54
35. G. Hu, R. D. Xu, S. W. He, B.M. Chen, H. T. Yang, B. H. Yu, and Q. Liu, *Trans. Nonferrous Metal. Soc. Ch.*, 25 (2015) 2095
36. S. He, R. Xu, G. Hu, and B. Chen, *RSC Adv.*, 6 (2016) 3362
37. P. Delahay, M. Pourbaix, and P. Van Rysselberghe, *J. Electrochem. Soc.*, 98 (1951) 57
38. C. J. Clarke, G. J. Browning, and S. W. Donne, *Electrochim. Acta*, 51 (2006) 5773
39. International Centre for Diffraction Data, Power Diffraction File, 2007, Pennsylvania, USA, card number 72-2440 for  $\alpha$ -PbO<sub>2</sub>
40. R. Inguanta, F. Vergottini, G. Ferrara, S. Piazza, and C. Sunseri, *Electrochim. Acta*, 55 (2010) 8556